Characterization of Tricoordinate Boron Chemical Shift Tensors: Definitive High-Field Solid-State NMR Evidence for Anisotropic Boron Shielding

David L. Bryce,[†] Roderick E. Wasylishen,*[,‡] and Myrlene Gee[†]

Departments of Chemistry, University of Alberta, E3-24 Chemistry Centre, Edmonton, Alberta, Canada T6G 2G2, and Dalhousie University, Halifax, Nova Scotia, Canada B3H 4J3

Received: November 7, 2000; In Final Form: January 5, 2001

Despite the large known chemical shift (CS) range for boron and the large number of ^{11}B NMR studies of glasses, no boron CS tensors have been characterized to date. We report the application of solid-state NMR techniques at moderate (9.4 T) and high (17.63 T) applied magnetic field strengths to the characterization of the boron CS tensors in trimesitylborane ($BMes_3$) and triphenyl borate ($B(OPh)_3$). The boron CS tensor of the former compound exhibits a remarkably large span, $\Omega = 121 \pm 1$ ppm, which encompasses the known range of isotropic chemical shifts for tricoordinate boron compounds. Conversely, the effect of the boron CS tensor on the ^{11}B NMR spectra of $B(OPh)_3$ is difficult to observe and quantify even at field strengths as high as 17.63 T; we find $\Omega \leq 10$ ppm. This marked difference in the boron nuclear magnetic shielding tensors is reproduced accurately by a series of ab initio and DFT calculations with a range of basis sets. The difference is rationalized in the context of Ramsey's theory of nuclear magnetic shielding by considering contributions to the paramagnetic shielding in the tricoordinate boron plane. Differences in the in-plane shielding tensor components for the molecules considered are a result of variations in the effectiveness of the mixing of occupied σ orbitals with virtual π orbitals under the influence of an applied magnetic field. A similar explanation has been invoked to rationalize ^{13}C isotropic chemical shifts in classical and nonclassical carbocations. We also report experimental and calculated boron nuclear quadrupolar coupling constants and asymmetry parameters for $BMes_3$ and $B(OPh)_3$. A combination of experimental and theoretical results provides the orientation of the CS and electric field gradient tensors in the molecular framework.

Introduction

The study of half-integer quadrupolar nuclei in the solid state via nuclear magnetic resonance (NMR) spectroscopy has advanced tremendously over the past decade.[1] New developments aimed at averaging or refocusing the quadrupolar interaction such as the multiple-quantum magic-angle-spinning (MQMAS) experiment[2] have allowed for the acquisition of "high-resolution" NMR spectra of half-integer quadrupolar nuclei, e.g., ^{11}B, ^{23}Na, ^{17}O, and ^{27}Al.[3,4] This is advantageous, for example, in the resolution of multiple magnetically or crystallographically nonequivalent nuclear sites. More recently, several groups have begun to explore NMR interactions traditionally only observed in the MAS spectra of spin-1/2 nuclei, which would previously have been obscured by the typically dominant quadrupolar interaction,[4] e.g., residual dipolar couplings between quadrupolar nuclei.

Although these subtle effects are now becoming observable using MQMAS methodology, these experiments are done under MAS conditions where the chemical shift (CS) tensor is averaged to its isotropic value. The CS tensor is arguably the most important NMR parameter. With commercially available magnetic field strengths, $\mathbf{B}_0$, ever-increasing, the influence of the CS tensor will become increasingly important since it scales linearly with $\mathbf{B}_0$. The magnitude and relative orientation of the CS tensors may be important, for example, in obtaining quantitative results from the rotational resonance[5] experiments recently introduced for half-integer quadrupolar nuclei,[6,7] especially for nuclei with relatively small or moderate quadrupole moments such as ^{11}B ($Q = 40.59$ mb).[8] An ongoing line of research in our group has been the characterization of chemical shift tensors of half-integer quadrupolar nuclei, e.g., cesium,[9] molybdenum,[10] aluminum,[11] copper,[12] and beryllium.[13] Here, we extend this work to boron.

Boron has a diverse structural chemistry and is particularly amenable to NMR studies. Of its two naturally occurring isotopes, ^{11}B ($I = 3/2$; NA = 80.42%; $\Xi = 32.09$ MHz) is best-suited to NMR spectroscopy. This is evidenced by the large number of isotropic shifts and indirect spin−spin coupling constants which have been reported.[14−18] In particular, many boron-containing glasses have been examined by ^{11}B NMR.[3g−i,19] The chemical shift range of boron in tricoordinate and tetracoordinate compounds extends over approximately 230 ppm.[18] Relatively recent work on metallaboranes[20] has extended this range to over 350 ppm.[21,22] Despite the surfeit of ^{11}B NMR data and the substantial range of chemical shifts, to date no boron CS tensor has been characterized.

In the present work, we report the first experimental characterization of a boron CS tensor. Boron-11 NMR spectroscopy of MAS and stationary solid powdered samples of crystalline trimesitylborane ($BMes_3$, Mes = 2,4,6-trimethylphenyl) and triphenyl borate ($B(OPh)_3$) has been carried out at applied magnetic field strengths of 17.63 and 9.4 T. From these experiments, both the boron chemical shift tensors and the

* To whom correspondence should be addressed at the University of Alberta. Phone: 780-492-4336. Fax: 780-492-8231. E-mail: Roderick.Wasylishen@UAlberta.Ca.
[†] Dalhousie University.
[‡] University of Alberta.

10.1021/jp004068c CCC: $20.00
Published on Web 03/15/2001

nuclear quadrupolar coupling parameters have been determined. Marked differences in the boron shift tensors in these two compounds are reproduced by ab initio and density functional theory calculations with a range of basis sets. Prompted by Olah's ^{13}C NMR studies of carbocations,[23] parallels between the ^{13}C isotropic chemical shifts of carbocations and the ^{11}B isotropic chemical shifts in analogous neutral compounds have been illustrated in the literature.[24] The ^{13}C shifts have been rationalized[25] in terms of the paramagnetic shielding term in Ramsey's theory of nuclear magnetic shielding.[26] Here, we extend this discussion to rationalize the difference between the boron CS tensors of boranes and borates.

Nuclear Magnetic Shielding and Quadrupolar Interactions: Equations and Definitions

The relevant interactions for an isolated quadrupolar nucleus such as ^{11}B in an external applied magnetic field have been described extensively in the literature.[27] Here, we present key concepts and definitions essential to the following discussion. In addition to the Zeeman interaction, we consider the quadrupolar and nuclear magnetic shielding interactions. For a stationary powdered sample, both of these interactions contribute to the observed spectrum. We may summarize the nuclear magnetic shielding and Zeeman Hamiltonians in a succinct form to give

$$\hat{H}_{Z,CS} = -\frac{\gamma h}{2\pi}[\mathbf{I}\cdot(\mathbf{l} - \boldsymbol{\sigma})\cdot\mathbf{B}_0] \quad (1)$$

where $\mathbf{B}_0$ is the external applied magnetic field, $\mathbf{l}$ is the unit tensor, γ is the magnetogyric ratio of the nucleus being observed, $\mathbf{I}$ is the nuclear spin angular momentum operator, and $\boldsymbol{\sigma}$ is the nuclear magnetic shielding tensor. We note that the influence of the shielding tensor scales linearly with $\mathbf{B}_0$. In its principal axis system, the symmetric part of the shielding tensor has three principal components designated as σ_{11}, σ_{22}, and σ_{33} where $\sigma_{11} \leq \sigma_{22} \leq \sigma_{33}$. The shielding tensor is directly related to the observable CS tensor by the following equation:

$$\delta_{ii,\text{sample}} = \frac{\sigma_{\text{iso,ref}} - \sigma_{ii,\text{sample}}}{1 - \sigma_{\text{iso,ref}}} \times 10^6 \text{ (ppm)} \quad (2)$$

Here, $ii = 11$, 22, 23, or iso. In the case of light nuclei, e.g., ^{11}B, the isotropic shielding constant of the reference is much less than unity, and so the relationship may be simplified to give

$$\delta_{ii,\text{sample}} \cong \sigma_{\text{iso,ref}} - \sigma_{ii,\text{sample}} \quad (3)$$

The principal components of the symmetric part of the CS tensor are designated and ordered as $\delta_{11} \geq \delta_{22} \geq \delta_{33}$. The orientations of the CS and nuclear magnetic shielding tensors are identical. The span of the nuclear magnetic shielding or CS tensor is defined as[28]

$$\Omega = \sigma_{33} - \sigma_{11} = \delta_{11} - \delta_{33} \quad (4)$$

The skew of the tensors is defined as[28]

$$\kappa = \frac{3(\sigma_{\text{iso}} - \sigma_{22})}{\Omega} = \frac{3(\delta_{22} - \delta_{\text{iso}})}{\Omega} \quad (5)$$

The skew is unitless and can take on values between -1 and $+1$.

For a nucleus such as ^{11}B in a stationary powdered sample, the quadrupolar interaction, given to first order by

$$\hat{H}_Q = h\frac{C_Q}{8I(2I-1)}(3\hat{I}_z^2 - \hat{\mathbf{I}}^2)(3\cos^2\theta - 1 + \eta\sin^2\theta\cos 2\phi) \quad (6)$$

must be considered in addition to the nuclear magnetic shielding interaction. The angles θ and ϕ define the orientation of $\mathbf{B}_0$ in the principal axis system of the electric field gradient (EFG) tensor in a manner analogous to that used for the nuclear magnetic shielding tensor. Under conditions of sufficiently rapid magic-angle spinning, the nuclear magnetic shielding and first-order quadrupolar interactions are averaged to their isotropic values and thus only the second-order quadrupolar interaction[1,27,29] needs to be considered. The components of the EFG tensor in its principal axis system are defined and ordered as follows:

$$|V_{zz}| \geq |V_{yy}| \geq |V_{xx}| \quad (7)$$

The quadrupolar coupling constant, C_Q, is given by

$$C_Q = \frac{eQV_{zz}}{h} \quad (8)$$

where e is the charge of an electron and Q is the nuclear quadrupole moment. The asymmetry parameter, η, is defined as

$$\eta = \frac{V_{xx} - V_{yy}}{V_{zz}} \quad (9)$$

Experimental and Computational Details

(i) Experimental Details.

Trimesitylborane (97%) and triphenyl borate were purchased from Aldrich and used without further purification. These compounds were powdered and packed in a glovebox under an inert atmosphere of nitrogen into 5 mm (Si_3N_3) and 4 mm (ZrO_2) rotors. Solid-state NMR experiments were carried out on Varian Inova ($\mathbf{B}_0 = 17.63$ T, $\nu_L(^{11}B) = 240.56$ MHz) and Bruker AMX ($\mathbf{B}_0 = 9.4$ T, $\nu_L(^{11}B) = 128.38$ MHz) spectrometers, with high-power proton decoupling. Referencing and setup were done using solid powdered sodium borohydride. Solid $NaBH_4$ has a chemical shift of -42.06 ppm relative to the ^{11}B standard, liquid $F_3B{\cdot}O(C_2H_5)_2$.[30] Chemical shifts reported herein are therefore with respect to liquid $F_3B{\cdot}O(C_2H_5)_2$ at 0.00 ppm. For MAS experiments, the magic angle was set using the ^{23}Na resonance of $NaNO_3$.[31] Recycle delays of 2−20 s were used. For stationary samples, both one-pulse and quadrupolar echo ($\pi/2-\tau_1-\pi-\tau_2-$ACQ)[27,32] experiments were carried out. Typical $\pi/2$ pulse lengths for solid $NaBH_4$ were 2.0−4.0 μs. For one-pulse experiments, pulses of length 1.0−1.5 μs were used. The probes used at both fields caused a background in the ^{11}B spectrum as a result of boron nitride in the stators. At 17.63 T, the intensity of this background was low compared with the signal of interest; the most effective method for removing it from spectra obtained without quadrupolar echoes was simply to subtract the spectrum of an empty rotor from the spectrum of interest. In contrast, at 9.4 T, the ^{11}B background due to the probe swamped the sample signal; the quadrupolar echo sequence proved most effective in this case for suppressing the background signal.

All spectra were analyzed and simulated using the WSOLIDS software package which was developed in our laboratory.[33] This package incorporates the space-tiling algorithm of Alderman et al. for the efficient generation of powder patterns.[34] For MAS

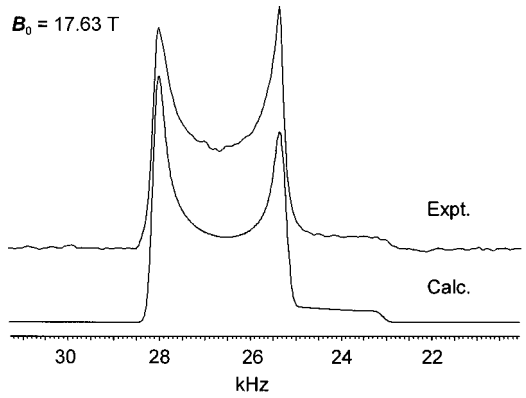

Figure 1. Boron-11 MAS NMR spectrum of solid powdered trimesitylborane along with the best-fit simulation using the parameters shown in Table 1. The experimental spectrum ($\mathbf{B}_0 = 17.63$ T, $\nu_L(^{11}B) = 240.56$ MHz) was acquired at an MAS rate of 10.5 kHz with a recycle delay of 5.0 s and is the sum of 2000 acquisitions. To obtain a second-order quadrupolar powder pattern near the limit of an infinite spinning rate, spinning sidebands were summed with the centerband to produce the spectrum shown here. The ^{11}B resonance of external solid $NaBH_4$ was set to 0 kHz.

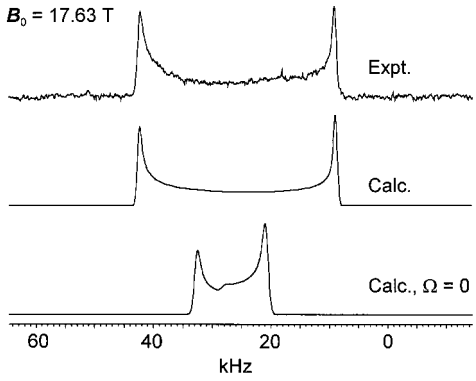

Figure 2. Boron-11 NMR spectrum of stationary solid powdered trimesitylborane along with the best-fit simulation using the parameters shown in Table 1. A span, Ω, of 121 ppm is used for the best-fit simulation. Also shown is the simulated spectrum obtained when the span is assumed to be zero. The experimental spectrum ($\mathbf{B}_0 = 17.63$ T, $\nu_L(^{11}B) = 240.56$ MHz) was obtained with a recycle delay of 2.0 s and is the sum of 2000 acquisitions. Background signal from the probe in the spectral region 0−20 kHz was subtracted from the original spectrum to give the result shown here. The ^{11}B resonance of external solid $NaBH_4$ was set to 0 kHz.

spectra, summation of spinning sidebands into the centerband was done using WINNMR.[35]

(ii) Computational Details.

All calculations of nuclear magnetic shielding and EFG tensors were carried out using Gaussian 98 for Windows[36] running on Dell Dimension computers (Pentium III, 550 MHz, 128 Mb RAM, and Pentium III, 866 MHz, 512 Mb RAM) or using Gaussian 98[36] on a 43P Model 260 IBM RS/6000 workstation with dual 200 MHz processors. The geometry used for the calculations on trimesitylborane was taken from X-ray diffraction atomic coordinates,[37] and the geometry for trimethyl borate was taken from electron diffraction atomic coordinates.[38] Carbon−hydrogen bond lengths were set to 1.09 Å.[39] Calculations of nuclear magnetic shielding tensors were done using the GIAO (gauge-including atomic orbitals) method.[40] For comparison, both the restricted Hartree−Fock (RHF) method and density functional theory (DFT) using the B3LYP functional[41] were employed for most calculations. Locally dense basis sets[42] were used for some calculations. All basis sets (3-21G, 6-31G, 6-311G*, 6-311++G**) were available within the Gaussian package.

The nuclear quadrupolar coupling constants, C_Q, were determined from the calculated largest EFG component, V_{zz}, by means of eq 8. Conversion of V_{zz} from atomic units to V m^{-2} was carried out by using the factor 9.7177×10^{21} V m^{-2} per atomic unit.[43] The accepted value of the nuclear quadrupole moment, Q, for ^{11}B is 40.59 mb.[8]

Results and Discussion

(i) Solid-State NMR.

Striking and definitive evidence for anisotropic boron shielding is found for trimesitylborane. Shown in Figures 1 and 2 are experimental spectra of magic-angle spinning and stationary powdered samples of trimesitylborane obtained with an external applied magnetic field of 17.63 T. Also shown are the best-fit simulated spectra, which were calculated using the parameters summarized in Table 1. The precision of these parameters was determined by analyzing spectra of MAS and stationary samples obtained at both 17.63 and 9.4 T (not shown). Under MAS conditions, the CS tensor is averaged to its isotropic value. We note that, for a quadrupolar nucleus, the observed center-of-gravity shift is the sum of the isotropic shift and a second-order quadrupolar shift.[44] The isotropic chemical shift, quadrupolar coupling constant, and asymmetry parameter were first determined from spectra of MAS samples (Figure 1). Since the simulated spectra assume an infinite spinning rate, spinning sidebands were summed into the centerband during processing of the experimental spectrum to allow for an appropriate comparison of experimental and simulated spectra. The isotropic shift, 77.4 ± 0.5 ppm, is similar to the value reported in $CDCl_3$ solution, 79.0 ppm.[45] A quadrupolar coupling constant of 4.75 MHz is in good agreement with the values determined for a series of trialkylboranes at 77 K via nuclear quadrupole resonance methods by Love[46] and discussed by Lucken;[47] for example, the quadrupolar coupling constant in trimethylborane is 4.876 MHz. For $B(Mes)_3$ at 17.63 T, the second-order quadrupolar shift is −2.3 kHz (−9.7 ppm). The asymmetry parameter, η, was determined to be zero. Townes−Dailey analysis[48] indicates that the asymmetry parameter should be zero for the central atom in an isolated trigonal planar compound;[47] the two in-plane components are equal. In the solid state, where crystal packing must be considered, it has been found experimentally that in some cases, e.g., triethylborane ($\eta = 0.009$), the asymmetry parameter can deviate very slightly from zero.[46,49] Consideration of the geometry about the boron atom in trimesitylborane[50] (space group $C2/c$, $Z = 4$), as indicated by the X-ray crystal structure,[37] shows that the boron atom and

TABLE 1: Experimental Boron-11 Chemical Shift Tensors and Quadrupolar Parameters for Trimesitylborane and Triphenyl Borate

	trimesitylborane	triphenyl borate
δ_{iso}/ppm[a]	77.4 ± 0.5	17.9 ± 0.5
Ω/ppm	121 ± 1	<10
κ	1.0	0.0 ± 0.3
C_Q/MHz	4.75 ± 0.01	2.32 ± 0.02
η	0.0	0.0
α	0	0[b]
β	0	0
γ	0	0

[a] With respect to liquid $F_3B{\cdot}OEt_2$ at 0.00 ppm (converted by subtracting 42.06 ppm from shift referenced to solid $NaBH_4$). [b] The Euler angles were set to zero for the best-fit simulation shown in Figure 4 although, given the small span of the shielding tensor, we cannot conclusively determine its orientation with respect to the EFG tensor.

one mesityl group lie on a 2-fold rotation axis; there is no true 3-fold symmetry. An idealized trimesitylborane molecule would have D_3 point group symmetry. From the experimental value of $\eta = 0$, we conclude that the largest component of the EFG tensor is perpendicular to the tricoordinate boron plane. This orientation is reproduced by ab initio calculations (vide infra).

Analysis of ^{11}B NMR spectra of stationary powdered trimesitylborane at 17.63 T (Figure 2) and 9.4 T (not shown) allows for the determination of the principal components of the boron chemical shift tensor ($\delta_{11} = \delta_{22} = 117.7$ ppm, $\delta_{33} = -3.3$ ppm) as well as its orientation relative to the EFG tensor. As shown in Figure 2 and Table 1, the span of the boron CS tensor was determined to be 121 ± 1 ppm. For comparison, a simulated spectrum for which the span was set to zero is also shown. Thus, at 17.63 T, where 121 ppm is equivalent to 29 kHz for ^{11}B, anisotropic shielding accounts for more than half of the total breadth (35 kHz) of the powder pattern! Parameters obtained from the best-fit simulated spectrum for trimesitylborane indicate that the CS tensor is coincident with the EFG tensor and that the skew, κ, of the CS tensor is 1.0. This means that the in-plane components of the CS tensor are equal, as is the case for the EFG tensor. Although the electric field gradient and nuclear magnetic shielding tensors are fundamentally different properties, in the case of trimesitylborane both of these tensors are oriented such that their largest components are coincident. This is not always the case, even in situations of relatively high symmetry.[11,13]

We are unaware of any other definitive reports of anisotropic boron shielding measured using experimental solid-state NMR techniques. Power has provided a qualitative estimate of the span of the boron CS tensor in solid $Ph_3P{\cdot}BH_3$ and finds it to be less than 50 ppm;[51] our own work on this compound indicates that the span is likely less than 30 ppm. We note that a span on the order of 200 ppm has been determined for gaseous BF[52] on the basis of the spin-rotation data of Cazzoli et al.[53] Spin-rotation data are also available for a series of linear boron-containing molecules, FBO, ClBO, and FBS, although the results have not been interpreted explicitly in terms of the span of the shielding tensor.[54,55] The spans of the boron shielding tensors for these three linear triatomic molecules, as derived from the spin-rotation data, are approximately 210−220 ppm.

The case of trimesitylborane represents a very clear example of anisotropic boron shielding. The horns of the stationary powder spectrum are very sharp. In particular, ^{11}B−^{11}B intermolecular homonuclear dipolar interactions are small due to the fact that the boron nucleus is quite sheltered from boron nuclei in adjacent molecules by the large mesityl groups. It has been our experience that this is not the case for many compounds for which one might expect to detect anisotropic boron shielding. Additionally, many trigonally coordinated boron atoms are bonded to nitrogen in compounds such as borazines. We have found that, under stationary conditions, heteronuclear ^{14}N−^{11}B dipolar interactions will cause the ^{11}B NMR spectrum to be broadened to an extent which renders the definitive characterization of boron CS tensors difficult even at field strengths as high as 17.63 T.

If compounds in which boron atoms may be subjected to significant ^{11}B−^{11}B homonuclear or ^{14}N−^{11}B heteronuclear dipolar couplings are excluded, other likely candidates for significant boron shielding anisotropy, beyond the boranes, are the borates, $B(OR)_3$. Shown in Figures 3 and 4 are the ^{11}B NMR spectra of MAS and stationary samples of solid powdered triphenyl borate along with best-fit simulations. As with trimesitylborane, the quadrupolar parameters (Table 1) were extracted from analysis of the spectra of MAS samples at 9.4 T (Figure 3) and 17.63 T (not shown). The quadrupolar coupling constant, 2.32 MHz, is less than half the value of that for trimesitylborane. This reduction upon moving from a triarylborane to a triaryl borate is supported by the measurements of Love,[46] e.g., $C_Q(^{11}B)$ for $B(OH)_3$ is 2.56 MHz. In sharp contrast to the spectrum of stationary trimesitylborane, that of triphenyl borate derives most of its breadth from the quadrupolar interaction (Figure 4). At 17.63 T, the total breadth is only about 6 kHz, compared to 35 kHz for trimesitylborane. The isotropic shift, 17.9 ± 0.5 ppm, is in good agreement with the value reported in solution, 16.5 ppm.[56] On the basis of the the best-fit parameters obtained from analyses of the spectrum shown in Figure 4 (17.63 T) and a spectrum acquired at 9.4 T (not shown), the span of the boron CS tensor was determined to be less than 10 ppm. Also shown is a simulated spectrum for which the span was assumed to be zero. Although the span is an order of magnitude less than in trimesitylborane, the results presented in Figure 4 demonstrate that the span of the boron CS tensor in triphenyl borate is certainly nonzero. The simulated spectrum is not very sensitive to the skew or the orientation of the CS tensor with respect to the EFG tensor, as is to be expected when the span is small. Thus, from the experimental data alone we

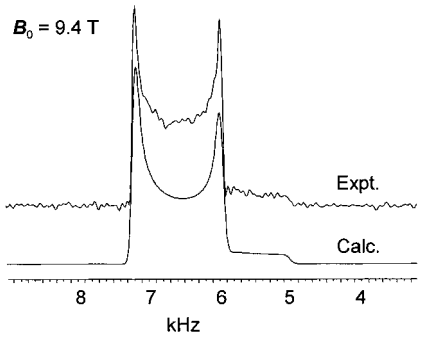

Figure 3. Boron-11 MAS NMR spectrum of solid powdered triphenyl borate along with the best-fit simulation using the parameters shown in Table 1. The experimental spectrum ($\mathbf{B}_0 = 9.4$ T, $\nu_L(^{11}B) = 128.3$ MHz) was acquired at an MAS rate of 9.0 kHz with a recycle delay of 10.0 s and is the sum of 5686 acquisitions. To observe this signal, a $\pi/2-\tau_1-\pi-\tau_2$ echo sequence was used to suppress the overwhelming background resonance from boron nitride in the probe stator. The ^{11}B resonance of external solid $NaBH_4$ was set to 0 kHz.

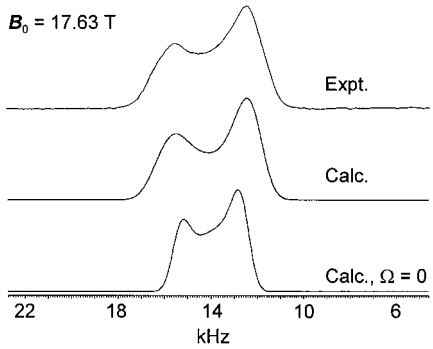

Figure 4. Boron-11 NMR spectrum of stationary solid powdered triphenyl borate along with the best-fit simulation using the parameters shown in Table 1. A span, Ω, of 8 ppm is used for the best-fit simulation. Also shown is the simulated spectrum obtained when the span is assumed to be zero. The experimental spectrum ($\mathbf{B}_0 = 17.63$ T, $\nu_L(^{11}B) = 240.56$ MHz) was obtained with a recycle delay of 20.0 s and is the sum of 128 acquisitions. Background signal from the probe in the spectral region 0−20 kHz was subtracted from the original spectrum to give the result shown here. The ^{11}B resonance of external solid $NaBH_4$ was set to 0 kHz.

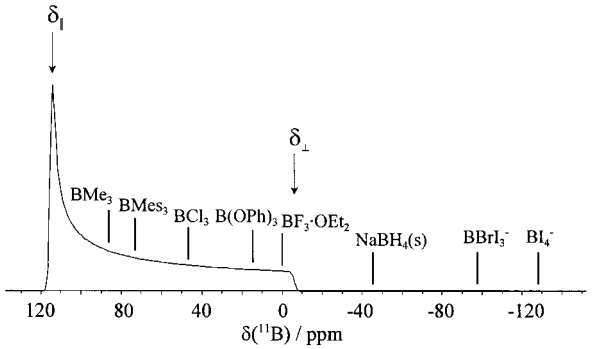

Figure 5. Boron chemical shift scale with representative compounds over the range of known isotropic chemical shifts for three- and four-coordinate boron. These data are from refs 14−18 except for $B(Mes)_3$ and $B(OPh)_3$ (this work). The usual reference is $F_3B{\cdot}O(C_2H_5)_2$ at 0.00 ppm. Also indicated is the boron chemical shift tensor in trimesitylborane. The span of this tensor, 121 ppm, covers the known range of isotropic shifts for tricoordinate boron. The component of the shift tensor which is perpendicular to the tricoordinate boron plane is denoted by $\delta_\perp$, and the two equivalent components which lie in this plane are designated by $\delta_{\parallel}$. Boron chemical shifts in some metallaboranes may be as high as 226 ppm, thereby extending the total boron shift range to over 350 ppm.

cannot conclusively determine the relative orientations of these tensors in triphenyl borate. However, given the coincident experimental orientation for trimesitylborane and results obtained from ab initio calculations (vide infra), it is likely that the largest component of the EFG and nuclear magnetic shielding tensors, V_{zz} and σ_{33}, are coincident.

The span of the boron CS tensor in triphenyl borate may be compared with those for the central atom in the analogous trigonally coordinated carbon and nitrogen moieties CO_3^{2-} and NO_3^-. The trend is that the span of the CS tensor of the central atom increases from boron ($\leq$10 ppm in $B(OPh)_3$) to carbon (75 ppm in $CaCO_3$)[57,58] to nitrogen (231 ppm in NH_4NO_3),[59] across the periodic table. A discussion of the carbon and nitrogen chemical shifts has been presented by Spiess.[58]

A selection of tricoordinate and tetracoordinate boron compounds and their isotropic chemical shifts are presented in Figure 5. The chemical shifts shown here bridge most of the known range. Also shown is the boron shift tensor for trimesitylborane. Clearly, this tensor spans the range of most tricoordinate boron isotropic chemical shifts. Metallaboranes are not represented on this chemical shift scale. Some metallaboranes exhibit isotropic boron chemical shifts as large as 226 ppm;[22] these are undoubtedly special compounds in which the boron nuclei are also expected to exhibit large shielding anisotropy.

(ii) Ab Initio Calculations.

The results of ab initio calculations of the ^{11}B nuclear magnetic shielding and EFG tensors in trimesitylborane are presented in Table 2. Since there is no absolute shielding scale for boron, we discuss the calculated nuclear magnetic shielding tensors in terms of their span and skew rather than their principal components to allow for comparison with experiment. A reliable absolute shielding scale for boron would allow for a direct comparison of the experimental and calculated principal components. The experimentally determined tensors are reproduced very well by the calculations. At the RHF/6-311G* level, a span of 117 ppm is predicted while the B3LYP functional with the same basis set gives a span of 127 ppm. Both of these results are in excellent agreement with the experimental value of 121 $\pm$ 1 ppm. Trimesitylborane is a moderately sized molecule with 61 atoms. Thus, the effect of locally dense basis sets was investigated, i.e., where the boron atom and the carbon atoms directly bonded to boron are represented by a relatively large basis set (6-311G* or 6-311++G** in this case) and the remaining atoms are represented by a relatively small basis set (3-21G in this case). Our results show a decrease in the calculated span, from 117 to 104 ppm for the RHF calculation and from 127 to 109 ppm for the DFT calculation. All of the calculations predict a skew of $\sim$0.9 for the boron shielding tensor, compared to the experimental value of 1.0. The predicted orientation of the shielding tensor is in agreement with the experimental chemical shift tensor orientation; δ_{33} is perpendicular to the tricoordinate boron plane (Figure 6), and the component of intermediate shielding, δ_{22}, lies along the molecular C_2 axis.

The calculations presented here have been carried out on single gas-phase molecules while the experiments are performed in the solid state. Thus, the good agreement between theory and experiment suggests that intermolecular interactions involving the boron nuclei are weak. Certainly the bulky trimesityl substituents hamper boron−boron interactions. Bailey has demonstrated the reliability of the B3LYP functional and the MP2 method for the calculation of quadrupolar coupling constants in small molecules in the gas phase, where intermolecular effects are relatively unimportant.[60] Our calculated quadrupolar coupling constants for trimesitylborane range from 4.26 to 5.44 MHz, and all are in reasonable accord with the experimental value of 4.75 MHz. We note that the addition of diffuse functions makes essentially no difference to the calculated quadrupolar coupling constants (e.g., 6-311G*/3-21G compared with 6-311++G**/3-21G). All the calculations presented here predict an asymmetry parameter of zero, in agreement with experiment. The calculated orientation is consistent with our experimental conclusion that V_{zz} is perpendicular to the tricoordinate boron plane (Figure 6). The results for trimesitylborane extend the good agreement between experimental and theoretical ^{11}B quadrupolar coupling constants obtained by Bailey.[60]

Crystal structure data are unavailable for triphenyl borate, and rather than using an ab initio optimized structure, we have carried out calculations on a model compound, trimethyl borate, for which electron diffraction data exist.[38] Quantitative agreement between experimental and theoretical results is thus not expected; however, distinct differences between the boron shielding tensors of boranes and borates is expected. The results of these calculations are summarized in Table 3. The calculated shielding tensors exhibit spans ranging from 0.9 ppm (B3LYP/6-311++G**) to 4.9 ppm (RHF/6-311++G**) and support the experimental observation that Ω is less than 10 ppm. The calculated skews are not very consistent as the basis set and/or method of calculation is altered, ranging from −0.88 to 0.93; however, this is not surprising for a shielding tensor with such a small span. Indeed, the experimental value of κ has a large uncertainty associated with it, 0.0 $\pm$ 0.3. While we have observed a very anisotropic boron CS tensor for trimesitylborane, the boron CS tensors of trialkyl and triaryl borates are fortuitously nearly isotropic. A relatively small span for trimethyl borate and a relatively large span for trimethylborane was predicted by Ebraheem and Webb in 1977 on the basis of the results of semiempirical CNDO/S calculations.[61] IGLO (individual gauge for localized orbitals) calculations on BF_3 indicate that the in-plane boron shift tensor components are actually larger than the unique component which is perpendicular to the molecular plane ($\kappa < 0$);[25] our own GIAO calculations also give a negative skew. This result implies that indeed the borates are

TABLE 2: Ab Initio and Density Functional Theory Calculations of the Boron-11 Nuclear Magnetic Shielding Tensor and Quadrupolar Coupling Parameters for Trimesitylborane

method	basis set[a]	σ_{iso}/ppm	Ω/ppm	κ	C_Q/MHz	η
RHF	6-31G	56	112	0.91	5.02	0.00
RHF	6-311G*/3-21G	66	104	0.90	4.63	0.00
RHF	6-311G*	46	117	0.91	5.44	0.00
RHF	6-311++G**/3-21G	65	104	0.90	4.62	0.00
DFT/B3LYP	6-31G	41	116	0.90	4.74	0.01
DFT/B3LYP	6-311G*/3-21G	54	109	0.88	4.26	0.01
DFT/B3LYP	6-311G*	28	127	0.89	5.23	0.00
DFT/B3LYP	6-311++G**/3-21G	54	109	0.88	4.26	0.01
expt[b]			121	1.00	4.75	0.00

[a] The first listed basis set was used on boron and the carbon atoms directly bonded to boron. The second basis set listed was used on all remaining atoms. Where only one basis set is listed, this was applied to all atoms. [b] Solid state (this work).

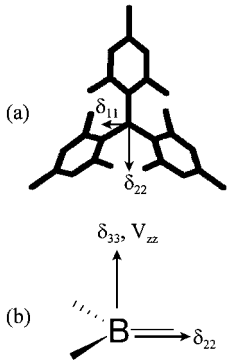

Figure 6. Calculated orientation of the boron chemical shift tensor and electric field gradient tensor in trimesitylborane. (a) View from above the tricoordinate boron plane. Both δ_{11} and δ_{22} lie in this plane. The intermediate shift component, δ_{22}, lies along a C_2 symmetry axis. (b) View along the tricoordinate boron plane. The δ_{33} and V_{zz} components are perpendicular to the tricoordinate boron plane. The EFG tensor is axially symmetric.

at a crossing-over point, where all three principal components of the boron CS tensor are serendipitously almost equal.

The calculated quadrupolar coupling constant for trimethyl borate, 2.25 MHz at the B3LYP/6-311++G** level, is in accord with the experimental value of 2.32 MHz in triphenyl borate. Once again, the asymmetry parameter is zero for all calculations. As for trimesitylborane, the calculations indicate that the largest component of the EFG tensor is perpendicular to the tricoordinate boron plane.

(iii) Rationalization of the Difference in Spans: Comparison with ^{13}C Shifts of Carbocations.

The explanation for the marked difference in the spans of the boron shielding tensors for a triarylborane compared to a triaryl borate is not immediately obvious. Both boron atoms are in symmetrical trigonal planar environments bonded to first-row elements. On the basis of symmetry considerations alone, one might expect the spans to be comparable. In the following section, ab initio calculations of the molecular electronic structures are presented and the difference in shielding tensors is rationalized in the context of Ramsey's theory of nuclear magnetic shielding.

Several reports have described apparent correlations between the ^{13}C isotropic chemical shifts of trigonal planar carbon-centered cations and the ^{11}B isotropic chemical shifts of analogous tricoordinate neutral boron compounds.[24] The IGLO ab initio method has been applied to the calculation of ^{13}C isotropic chemical shifts in various classical and nonclassical carbocations.[25,62] Kutzelnigg has presented an explanation for the large range of values for $\delta_{iso}(^{13}C)$.[25] In the context of Ramsey's theory, the nuclear magnetic shielding tensor may be decomposed into diamagnetic (σ^d) and paramagnetic (σ^p) contributions. For nuclei other than hydrogen, generally the paramagnetic term is the dominant factor in determining the anisotropy of the shielding tensor.[63]

When virtual "rotation" of an occupied MO results in favorable overlap of this MO with a low-lying virtual MO, paramagnetic deshielding is observed for the direction of the axis of rotation. For example, in classical carbocations, rotation of occupied bonding orbitals about any direction in the plane of the carbocation leads to favorable overlap with an empty p_z orbital which resides on the central carbon atom. This $\sigma \rightarrow \pi^*$ magnetic dipole allowed transition is of primary importance in determining the magnitude of the in-plane tensor components and, consequently, the isotropic chemical shift. For nonclassical carbocations, the p_z orbital is involved in bonding and thus is not available for the rotation of charge described above. Accordingly, nonclassical carbocations have smaller isotropic chemical shifts than do classical carbocations. The difference in energy between the ground state and excited singlet states is critical in deciding which virtual "rotations" will be important in determining σ^p. The closer in energy the occupied and virtual orbitals involved in the rotation are, the greater the (usually negative) paramagnetic contribution will be.

Comparison of the ab initio calculated boron shielding tensors in trimesitylborane and trimethyl borate indicates that the component perpendicular to the tricoordinate plane, $\sigma_\perp$, varies little compared to the in-plane shielding components. For example, at the RHF/6-311G* level, $\sigma_\perp$ is 122 ppm for trimesitylborane and 96 ppm for trimethyl borate. The average of the in-plane components, however, increases from 8 ppm in the borane to 101 ppm in the borate. As for carbocations, it is clear that the in-plane components are those which vary the most drastically from compound to compound and *thus these components determine the overall span of the shielding tensor as well as the isotropic shielding*. Tricoordinate boron compounds such as triarylboranes and triaryl borates also have a virtual p_z orbital available for magnetic dipole allowed transitions (rotations) which resides on boron. From a qualitative point of view, in borates the lone pairs on oxygen may be considered to donate strongly into the vacant orbital on boron, thus reducing its availability for the charge rotation discussed above. This would result in a reduction of σ^p. From a more quantitative standpoint, ab initio calculations (RHF/6-311G**) of the molecular orbitals for $B(CH_3)_3$ and $B(OH)_3$ in the C_{3h} point group reveal that the $e' \rightarrow a''$ ($\sigma \rightarrow \pi^*$) transition, which involves the requisite rotation about an axis in the plane of the tricoordinate boron (Figure 7), has a smaller energy gap in the borane (0.59405 hartree) than in $B(OH)_3$ (0.80555 hartree). Thus, we invoke the same explanation to rationalize the drastic difference between the boron CS tensors for trimesitylborane and triphenyl borate which we have observed experimentally. The boron

TABLE 3: Ab Initio and Density Functional Theory Calculations of the Boron-11 Nuclear Magnetic Shielding Tensor and Quadrupolar Coupling Parameters for Trimethyl Borate as a Model for Triphenyl Borate

method	basis set	σ_{iso}/ppm	Ω/ppm	κ	C_Q/MHz	η
RHF	6-311G	99	2.9	0.58	2.75	0.00
RHF	6-311++G**	100	4.9	−0.88	2.93	0.00
DFT/B3LYP	6-311G	86	4.7	0.93	1.90	0.00
DFT/B3LYP	6-311++G**	85	0.9	0.02	2.25	0.00
expt[64] $(B(OH)_3)$[a]					2.56	0.00[b]
expt[c] (triphenyl borate)			≤10	0.0 ± 0.3	2.32	0.00

[a] Solid state. [b] Assumed in original references. [c] Solid state (this work).

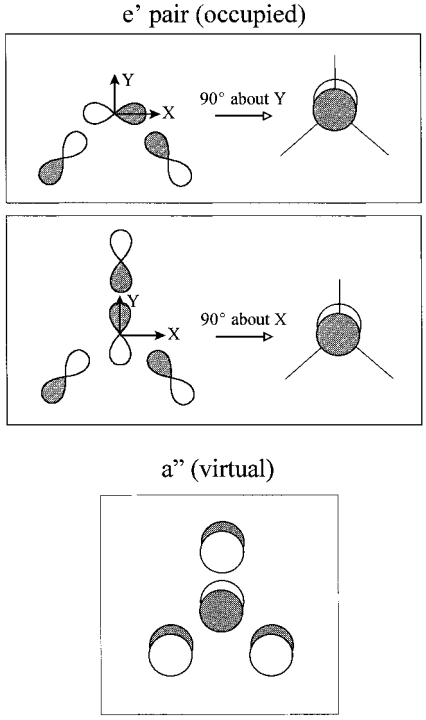

Figure 7. Molecular orbitals involved in $\sigma \rightarrow \pi^*$ magnetic dipole allowed transitions for planar tricoordinate boron compounds or carbocations in the C_{3h} space group, e.g., BMe_3 and $B(OH)_3$. The occupied degenerate e′ pair orbitals on the left lie in the tricoordinate boron plane. Focusing solely on the central atom, rotation of the top e′ orbital 90° about Y gives an orbital which overlaps constructively at boron with the virtual a″ orbital shown at the bottom. Similarly, the second e′ orbital may be rotated about X by 90° to give favorable overlap with a″ at boron.

nuclei in 4-coordinate boron compounds have smaller isotropic chemical shifts due to their different electronic structures, most importantly the lack of a virtual p_z orbital.

Conclusions

The present work has provided the first experimental characterization of a boron chemical shift tensor, for trimesitylborane. In analogy with ^{13}C chemical shifts of carbocations, it has also been shown that the in-plane ^{11}B chemical shift tensor components, which are largely responsible for differences in the isotropic chemical shift and the span of the shift tensor, vary greatly between boranes and borates. Ab initio and density functional theory calculations have been used to reproduce accurately the chemical shift tensor in trimesitylborane. Experimental characterization of the boron chemical shift tensor for triphenyl borate is less precise; the very small spans and the range of skews predicted by the ab initio calculations support our observation that the span of the boron shift tensor is very small in borates. This last point is pertinent to ^{11}B NMR studies of borate glasses, especially under stationary conditions. Finally, we wish to point out the need for a reliable absolute boron nuclear magnetic shielding scale. Such a scale would allow for more insightful comparisons between experimental chemical shift tensors and calculated nuclear magnetic shielding tensors.

Acknowledgment. The authors thank the solid-state NMR group at the University of Alberta and Dr. Mike Lumsden at Dalhousie University for many helpful comments. We thank Prof. Gang Wu at Queen's University for valuable suggestions. Part of this research was performed in the Environmental Molecular Sciences Laboratory (a national scientific user facility sponsored by the U.S. DOE Office of Biological and Environmental Research) located at Pacific Northwest National Laboratory, operated by Battelle for the DOE. We are very grateful to the staff at the EMSL for their assistance with the 17.63 T NMR system. We thank the Natural Sciences and Engineering Research Council of Canada (NSERC) for research grants. Some spectra (9.4 T) were acquired at the Atlantic Region Magnetic Resonance Centre, which is supported by NSERC. D.L.B. and M.G. thank NSERC, Dalhousie University, the Izaak Walton Killam Trust, and the Walter C. Sumner Foundation for postgraduate scholarships.

References and Notes

(1) Smith, M. E.; van Eck., E. R. H. *Prog. Nucl. Magn. Reson. Spectrosc.* **1999**, *34*, 159.

(2) (a) Medek, A.; Harwood, J. S.; Frydman, L. *J. Am. Chem. Soc.* **1995**, *117*, 12779. (b) Medek, A.; Frydman, L. *J. Braz. Chem. Soc.* **1999**, *10*, 263.

(3) For recent examples, see: (a) Wu, G. *Biochem. Cell Biol.* **1998**, *76*, 429. (b) Kanehashi, K.; Saito, K.; Sugisawa, H. *Chem. Lett.* **2000**, *6*, 588. (c) Bull, L. M.; Bussemer, B.; Anupõld, T.; Reinhold, A.; Samoson, A.; Sauer, J.; Cheetham, A. K.; Dupree, R. *J. Am. Chem. Soc.* **2000**, *122*, 4948. (d) Smith, L. J.; Eckert, H.; Cheetham, A. K. *J. Am. Chem. Soc.* **2000**, *122*, 1700. (e) Bodart, P. R.; Amoureux, J. P.; Pruski, M.; Bailly, A.; Fernandez, C. *Magn. Reson. Chem.* **1999**, *37*, S69. (f) Wang, S. H.; Stebbins, J. F. *J. Am. Ceram. Soc.* **1999**, *82*, 1519. (g) Hwang, S.-J.; Fernandez, C.; Amoureux, J. P.; Han, J.-W.; Cho, J.; Martin, S. W.; Pruski, M. *J. Am. Chem. Soc.* **1998**, *120*, 7337. (h) Stebbins, J. F.; Zhao, P. D.; Kroeker, S. *Solid State Nucl. Magn. Reson.* **2000**, *16*, 9. (i) Hwang, S.-J.; Fernandez, C.; Amoureux, J. P.; Cho, J.; Martin, S. W.; Pruski, M. *Solid State Nucl. Magn. Reson.* **1997**, *8*, 109.

(4) (a) Chan, J. C. C. *J. Magn. Reson.* **1999**, *140*, 487. (b) Pruski, M.; Bailly, A.; Lang, D. P.; Amoureux, J. P.; Fernandez, C. *Chem. Phys. Lett.* **1999**, *307*, 35. (c) Wu, G.; Yamada, K. *Chem. Phys. Lett.* **1999**, *313*, 519. (d) Wu, G. *Chem. Phys. Lett.* **2000**, *322*, 513. (e) Wi, S.; Frydman, L. *J. Chem. Phys.* **2000**, *112*, 3248. (f) Wu, G.; Wasylishen, R. E. *Mol. Phys.* **1998**, *95*, 1177.

(5) Bryce, D. L.; Wasylishen, R. E. In *Encyclopedia of Spectroscopy and Spectrometry*; Lindon, J. C., Tranter, G. E., Holmes, J. L., Eds.; Academic Press Ltd.: London, 2000; pp 2136−2144.

(6) Baldus, M.; Rovnyak, D.; Griffin, R. G. *J. Chem. Phys.* **2000**, *112*, 5902.

(7) Nijman, M.; Ernst, M.; Kentgens, A. P. M.; Meier, B. H. *Mol. Phys.* **2000**, *98*, 161.

(8) (a) Sundholm, D.; Olsen, J. *J. Chem. Phys.* **1991**, *94*, 5051. (b) Pyykkö, P. *Z. Naturforsch.* **1992**, *47a*, 189.

(9) Power, W. P.; Mooibroek, S.; Wasylishen, R. E.; Cameron, T. S. *J. Phys. Chem.* **1994**, *98*, 1552.

(10) Eichele, K.; Wasylishen, R. E.; Nelson, J. H. *J. Phys. Chem. A* **1997**, *101*, 5463.

(11) Schurko, R. W.; Wasylishen, R. E.; Foerster, H. *J. Phys. Chem. A* **1998**, *102*, 9750.
(12) Kroeker, S.; Wasylishen, R. E. *Can. J. Chem.* **1999**, *77*, 1962.
(13) Bryce, D. L.; Wasylishen, R. E. *J. Phys. Chem. A* **1999**, *103*, 7364.
(14) Mann, B. E. In *NMR and the Periodic Table*; Harris, R. K., Mann, B. E., Eds.; Academic Press: London, 1978; Section 4C.
(15) Kennedy, J. D. In *Multinuclear NMR*; Mason, J., Ed.; Plenum Press: New York, 1987; Chapter 8.
(16) Kidd, R. G. In *NMR of Newly Accessible Nuclei: Chemically and Biochemically Important Elements*; Laszlo, P., Ed.; Academic Press: New York, 1983; Vol. 2, Chapter 3.
(17) Wrackmeyer, B. In *Annual Reports on NMR Spectroscopy*; Webb, G. A., Ed.; Academic Press: London, 1988; Vol. 20, pp 61−203.
(18) Nöth, H.; Wrackmeyer, B. In *NMR Basic Principles and Progress*; Diehl, P., Fluck, E., Kosfeld, R., Eds.; Springer-Verlag: Berlin, 1978; Vol. 14.
(19) See for example: (a) Bray, P. J. *Inorg. Chim. Acta* **1999**, *289*, 158. (b) Eckert, H. *Prog. Nucl. Magn. Reson. Spectrosc.* **1992**, *24*, 159. (c) Chan, J. C. C.; Bertmer, M.; Eckert, H. *J. Am. Chem. Soc.* **1999**, *121*, 5238. (d) Bray, P. J.; Petersen, G. L. *Z. Naturforsch.* **1998**, *53a*, 273. (e) Kirkpartick, R. J.; Brow, R. K. *Solid State Nucl. Magn. Reson.* **1995**, *5*, 9. (f) Youngman, R. E.; Zwanziger, J. W. *J. Am. Chem. Soc.* **1995**, *117*, 1397. (g) van Wüllen, L.; Züchner, L.; Müller-Warmuth, W.; Eckert, H. *Solid State Nucl. Magn. Reson.* **1996**, *6*, 203. (h) van Wüllen, L.; Gee, B.; Züchner, L.; Bertmer, M.; Eckert, H. *Ber. Bunsen-Ges. Phys. Chem.* **1996**, *100*, 1539. (i) Bertmer, M.; Züchner, L.; Chan, J. C. C.; Eckert, H. *J. Phys. Chem. B* **2000**, *104*, 6541. (j) Chan, J. C. C.; Bertmer, M.; Eckert, H. *Chem. Phys. Lett.* **1998**, *292*, 154. (k) Silver, A. H.; Bray, P. J. *J. Chem. Phys.* **1958**, *29*, 984.
(20) For a review of metallaborane chemistry, see: Fehlner, T. P. *Organometallics* **2000**, *19*, 2643.
(21) Fehlner, T. P. *Collect. Czech. Chem. Commun.* **1999**, *64*, 767.
(22) (a) Khattar, R.; Puga, J.; Fehlner, T. P.; Rheingold, A. L. *J. Am. Chem. Soc.* **1989**, *111*, 1877. (b) Rath, N. P.; Fehlner, T. P. *J. Am. Chem. Soc.* **1987**, *109*, 5273. (c) Housecroft, C. E.; Buhl, M. L.; Long, G. J.; Fehlner, T. P. *J. Am. Chem. Soc.* **1987**, *109*, 3323. (d) Miller, V. R.; Weiss, R.; Grimes, R. N. *J. Am. Chem. Soc.* **1977**, *99*, 5646. (e) Venable, T. L.; Grimes, R. N. *Inorg. Chem.* **1982**, *21*, 887. (f) Lei, X.; Shang, M.; Fehlner, T. P. *J. Am. Chem. Soc.* **1999**, *121*, 1275. (g) Bandyopadhyay, A.; Shang, M.; Jun, C. S.; Fehlner, T. P. *Inorg. Chem.* **1994**, *33*, 3677. (h) Lei, X.; Shang, M.; Fehlner, T. P. *Inorg. Chem.* **1998**, *37*, 3900.
(23) (a) Olah, G. A. *Angew. Chem., Intl. Ed. Engl.* **1973**, *12*, 173. (b) Olah, G. A. *Angew. Chem., Intl. Ed. Engl.* **1995**, *34*, 1393.
(24) (a) Olah, G. A.; Rasul, G.; Surya Prakash, G. K. *J. Org. Chem.* **2000**, *65*, 5956. (b) Nöth, H.; Wrackmeyer, B. *Chem. Ber.* **1974**, *107*, 3070. (c) Spielvogel, B. F.; Nutt, W. R.; Izydore, R. A. *J. Am. Chem. Soc.* **1975**, *97*, 1609. (d) Wrackmeyer, B. *Z. Naturforsch.* **1980**, *35b*, 439.
(25) Kutzelnigg, W.; Fleischer, U.; Schindler, M. In *NMR Basic Principles and Progress*; Diehl, P., Fluck, E., Günther, H., Kosfeld, R., Seelig, J., Eds.; Springer-Verlag: Berlin, 1991; Vol. 23, pp 165−262.
(26) (a) Ramsey, N. F. *Phys. Rev.* **1950**, *77*, 567. (b) Ramsey, N. F. *Phys. Rev.* **1950**, *78*, 699. (c) Grutzner, J. B. In *Recent Advances in Organic NMR Spectroscopy*; Lambert, J. B., Rittner, R., Eds.; Norell Press: Landisville, NJ, 1987; Chapter 2.
(27) Freude, D.; Haase, J. In *NMR Basic Principles and Progress*; Diehl, P., Fluck, E., Günther, H., Kosfeld, R., Seelig, J., Eds.; Springer-Verlag: Berlin, 1993; Vol.29, pp 1−90.
(28) Mason, J. *Solid State Nucl. Magn. Reson.* **1993**, *2*, 285.
(29) Taulelle, F. In *Multinuclear Magnetic Resonance in Liquids and Solids-Chemical Applications*; Granger, P., Harris, R. K., Eds.; Kluwer Academic Publishers: Dordrecht, The Netherlands, 1990; pp 393−407.
(30) Hayashi, S.; Hayamizu, K. *Bull. Chem. Soc. Jpn.* **1989**, *62*, 2429.
(31) Jakobsen, H. J.; Skibsted, J.; Bildsøe, H.; Nielsen, N. C. *J. Magn. Reson.* **1989**, *85*, 173.
(32) Hahn, E. L. *Phys. Rev.* **1950**, *80*, 580.
(33) Eichele, K.; Wasylishen, R. E. *WSOLIDS NMR Simulation Package*, Version 1.17.26; 2000.
(34) Alderman, D. W.; Solum, M. S.; Grant, D. M. *J. Chem. Phys.* **1986**, *84*, 3717.
(35) *WIN NMR*, version 6.0; Bruker-Franzen Analytik GmbH, Germany.
(36) Frisch, M. J.; Trucks, G. W.; Schlegel, H. B.; Scuseria, G. E.; Robb, M. A.; Cheeseman, J. R.; Zakrzewski, V. G.; Montgomery, J. A., Jr.; Stratmann, R. E.; Burant, J. C.; Dapprich, S.; Millam, J. M.; Daniels, A. D.; Kudin, K. N.; Strain, M. C.; Farkas, O.; Tomasi, J.; Barone, V.; Cossi, M.; Cammi, R.; Mennucci, B.; Pomelli, C.; Adamo, C.; Clifford, S.; Ochterski, J.; Petersson, G. A.; Ayala, P. Y.; Cui, Q.; Morokuma, K.; Malick, D. K.; Rabuck, A. D.; Raghavachari, K.; Foresman, J. B.; Cioslowski, J.; Ortiz, J. V.; Stefanov, B. B.; Liu, G.; Liashenko, A.; Piskorz, P.; Komaromi, I.; Gomperts, R.; Martin, R. L.; Fox, D. J.; Keith, T.; Al-Laham, M. A.; Peng, C. Y.; Nanayakkara, A.; Gonzalez, C.; Challacombe, M.; Gill, P. M. W.; Johnson, B. G.; Chen, W.; Wong, M. W.; Andres, J. L.; Head-Gordon, M.; Replogle, E. S.; Pople, J. A. *Gaussian 98*, revision A.7; Gaussian, Inc.: Pittsburgh, PA, 1998.
(37) Blount, J. F.; Finocchiaro, P.; Gust, D.; Mislow, K. *J. Am. Chem. Soc.* **1973**, *95*, 7019.
(38) Gundersen, G.; Jonvik, T.; Seip, R. *Acta Chem. Scand. A* **1981**, *35*, 325.
(39) Jeffrey, G. A.; Ruble, J. R.; McMullan, R. K.; Pople, J. A. *Proc. R. Soc. London A* **1987**, *414*, 47.
(40) (a) Ditchfield, R. *Mol. Phys.* **1974**, *27*, 789. (b) Wolinski, K.; Hinton, J. F.; Pulay, P. *J. Am. Chem. Soc.* **1990**, *112*, 8251.
(41) Becke, A. D. *J. Chem. Phys.* **1993**, *98*, 5648.
(42) (a) Chesnut, D. B.; Moore, K. D. *J. Comput. Chem.* **1989**, *10*, 648. (b) Chesnut, D. B.; Rusiloski, B. E.; Moore, K. D.; Egolf, D. A. *J. Comput. Chem.* **1993**, *14*, 1364.
(43) Mills, I.; Cvitaš, T.; Homann, K.; Kallay, N.; Kuchitsu, K. *Quantities, Units and Symbols in Physical Chemistry*, 2nd ed.; International Union of Pure and Applied Chemistry Physical Chemistry Division, Blackwell Science: Oxford, U.K., 1993.
(44) Samoson, A. *Chem. Phys. Lett.* **1985**, *119*, 29.
(45) Brown, N. M. D.; Davidson, F.; Wilson, J. W. *J. Organomet. Chem.* **1981**, *209*, 1.
(46) Love, P. *J. Chem. Phys.* **1963**, *39*, 3044.
(47) Lucken, E. A. C. *Nuclear Quadrupole Coupling Constants*; Academic Press: London, 1969; Chapter 12.
(48) Townes, C. H.; Dailey, B. P. *J. Chem. Phys.* **1949**, *17*, 782.
(49) Dehmelt, H. G. *Z. Phys.* **1952**, *133*, 528.
(50) Although individual trimesitylborane molecules are chiral, the crystals are racemic due to their mirror plane symmetry.
(51) Power, W. P. *J. Am. Chem. Soc.* **1995**, *117*, 1800.
(52) Wasylishen, R. E.; Bryce, D. L.; Evans, C. J.; Gerry, M. C. L. *J. Mol. Spectrosc.* **2000**, *204*, 184.
(53) Cazzoli, G.; Cludi, L.; Degli Esposti, C.; Dore, L. *J. Mol. Spectrosc.* **1989**, *134*, 159.
(54) Gatehouse, B.; Müller, H. S. P.; Gerry, M. C. L. *J. Mol. Spectrosc.* **1998**, *190*, 157.
(55) Gatehouse, B. *Chem. Phys. Lett.* **1998**, *288*, 698.
(56) Henderson, W. G.; Mooney, E. F. In *Annual Review of NMR Spectroscopy*; Mooney, E. F., Ed.; Academic Press: London, 1969; Vol. 2, p 219.
(57) Lauterbur, P. C. *Phys. Rev. Lett.* **1958**, *1*, 343.
(58) Spiess, H. W. In *NMR Basic Principles and Progress*; Diehl, P., Fluck, E., Kosfeld, R., Eds.; Springer-Verlag: Berlin, 1978; Vol. 15, pp 55−214.
(59) (a) Gibby, M. G.; Griffin, R. G.; Pines, A.; Waugh, J. S. *Chem. Phys. Lett.* **1972**, *17*, 80. (b) Anderson-Altmann, K. L.; Grant, D. M. *J. Phys. Chem.* **1993**, *97*, 11096. This paper gives nitrate nitrogen CS tensor principal components for five solid phases of NH_4NO_3. We discuss the span for phase IV, at 18 °C, 231 ppm.
(60) Bailey, W. C. *J. Mol. Spectrosc.* **1997**, *185*, 403.
(61) Ebraheem, K. A. K.; Webb, G. A. *Org. Magn. Reson.* **1977**, *10*, 258.
(62) Schindler, M. *J. Am. Chem. Soc.* **1987**, *109*, 1020.
(63) Jameson, C. J.; Gutowsky, H. S. *J. Chem. Phys.* **1964**, *40*, 1714.
(64) (a) Bray, P. J.; Edwards, J. O.; O'Keefe, J. G.; Ross, V. F.; Tatsuzaki, I. *J. Chem. Phys.* **1961**, *35*, 435. (b) Silver, A. H. *J. Chem. Phys.* **1960**, *32*, 959.